Reports

Precision Lattice-Parameter Determination of $(Mg,Fe)SiO_3$ Tetragonal Garnets

RIE MATSUBARA, HIDEO TORAYA, SATOSHI TANAKA,* HIROSHI SAWAMOTO

The tetragonal garnet $(Mg,Fe)SiO_3$ is a high-pressure phase of pyroxene that is thought to be a major constituent of the earth's upper mantle. Its crystal structure is similar to that of cubic garnet, but it is slightly distorted to tetragonal symmetry so that its x-ray powder diffraction pattern shows a very small line splitting. A suite of tetragonal garnets with different compositions in the $MgSiO_3$-rich portion of the $MgSiO_3$-$FeSiO_3$ system was synthesized at about 20 gigapascals and 2000°C. The lattice parameters a and c of quenched samples were determined by whole-powder-pattern decomposition analysis of Fe Kα x-ray powder diffraction data, which has the capacity to resolve to a high degree heavily overlapping reflections. It was found that the lattice parameters can be obtained from the following equations: a (in angstroms) = 11.516 + 0.088x and c (in angstroms) = 11.428 + 0.157x, where x, the mole fraction of $FeSiO_3$, is $0.0 \leq x \leq 0.2$.

BECAUSE $(Mg,Fe)SiO_3$ PYROXENES are abundant minerals in the upper mantle, many investigators have studied the stability relations and the chemical and physical properties of the high-pressure and high-temperature phases of these pyroxenes to understand the deeper regions of the mantle. In these investigations, $MgSiO_3$ pyroxene (enstatite) was found to dissolve extensively in $Mg_3Al_2Si_3O_{12}$ garnet (pyrope) above 10 GPa and at about 1000°C. The existence of pure $MgSiO_3$ garnet with the structural formula $Mg_3{}^{VIII}(MgSi)^{VI}Si_3{}^{IV}O_{12}$, where the superscripts stand for coordination numbers, was inferred (*1*). Much higher temperature is required to synthesize $MgSiO_3$ garnet, and this was indeed accomplished at about 20 GPa and 2000°C by Kato and Kumazawa (*2*).

This $MgSiO_3$ garnet showed low birefringence under microscopic examination and slight line splitting of x-ray powder diffraction patterns, indicating that it does not have the cubic structure of true garnet but has a garnet-like structure with lower symmetry than cubic. Of the derivative structures of garnets, the tetragonal structure type with space group $I4_1/a$ is known for the high-pressure phase of $MnSiO_3$ (*3*), $CdGeO_3$, and $GaGeO_3$ (*4*). $MgSiO_3$ garnet was also thought to be isotypic to them. This was recently confirmed by the refinement of single-crystal x-ray diffraction data (*5*). The small distortions of the crystal structures of these tetragonal garnets from the cubic garnet structure are ascribed to the ordering of two kinds of cations in the octahedral sites.

For lattice-parameter determination from a powder pattern, individual profile fitting is the most common analytical method used. In this method, a least-squares curve-fitting is applied to the diffraction peaks in the selected 2θ range individually (θ is the Bragg angle), and their diffraction angles are determined. Then the lattice parameters are calculated from the resulting diffraction angles, again by a least-squares method. It is very difficult to resolve heavily overlapping peaks of the tetragonal garnet and to determine its lattice parameters precisely by the use of such a method.

One of the more advanced methods for lattice-parameter determination is the whole-powder-pattern decomposition (WPPD) method (*6, 7*), which is based on the assumption that the profile shape of reflection peaks and background level have some sort of angular dependence and the integrated intensities of the individual peaks are independent variables. The positions of all reflections are constrained by a set of lattice parameters, and with this method it is possible to decompose the whole diffraction pattern into its component reflections at a stroke to obtain lattice parameters of high accuracy by refining all reflections simultaneously. We have performed WPPD analyses on relatively good-quality x-ray powder data for a small amount of sample and have determined precise lattice parameters of tetragonal garnets with the compositions $MgSiO_3$, $(Mg_{0.90}Fe_{0.10})SiO_3$, and $(Mg_{0.81}Fe_{0.19})SiO_3$.

Starting materials with compositions $(Mg_{0.9}Fe_{0.1})SiO_3$ and $(Mg_{0.8}Fe_{0.2})SiO_3$ were prepared as follows. Stoichiometric (except for oxygen) powder mixtures of MgO (periclase), Fe_2O_3 (hematite), and SiO_2 (vitreous silica) were pelletized and then heated at about 1300°C for 20 to 30 hours in the flow of an H_2-CO_2 gas mixture (partial pressure ratio $p_{H_2}/p_{CO_2} \sim 1/2$). At this stage, the reduction of iron from Fe^{3+} to Fe^{2+} was completed and the formation of pyroxene had started. After quenching of the first stage, the samples were ground, pelletized, and heated to about 1300°C for 70 to 80 hours in H_2-CO_2 gas. The starting materials were checked by x-ray powder diffraction and optical microscopy. The x-ray powder diffraction pattern showed that they consisted primarily of protopyroxene and orthopyroxene with a small amount of clinopyroxene. Optical microscopy revealed the existence of a minor amount (approximately 1% by volume) of an isotropic substance with a much lower refractive index than that of pyroxene. This substance is thought to be surplus vitreous silica. The starting material of pure $MgSiO_3$ composition was synthesized from a stoichiometric

Table 1. X-ray data and details of the WPPD analyses.

Composition [x = Fe/(Fe + Mg)]*	2θ scan range (deg)	Maximum step intensities† (counts)	Minimum step intensities (counts)	Number of: Reflections used for refinement	Number of: "Zero-intensity" reflections‡	R_{wp} (%)
0.00(0)	21.0–98.8	26,166	470	99	34	4.7
0.10(1)	21.0–99.0	22,727	1,109	99	37	3.0
0.19(1)	22.0–98.8	13,496	875	61	19	3.5

*Electron probe microanalyses of the run products. The values given in parentheses are SDs in the least significant digit. †Peak maximum intensities of the most intense lines of tetragonal garnets. ‡See text.

R. Matsubara, S. Tanaka, H. Sawamoto, Department of Earth Sciences, Nagoya University, Nagoya 464-01, Japan.
H. Toraya, Ceramic Engineering Research Laboratory, Nagoya Institute of Technology, Tajimi 507, Japan.

*Present address: Institute of Space and Astronautical Science, Sagamihara 229, Japan.

powder mixture of MgO and SiO_2 at 1800°C and 200 bars. The x-ray diffraction pattern showed that the synthesized $MgSiO_3$ is a mixture of orthopyroxene and clinopyroxene.

The (Mg,Fe)SiO_3 garnets were synthesized at Nagoya University with an MA8-type high-pressure apparatus (*8*). The pressure was calibrated at room temperature with fixed points based on the abrupt changes in electrical resistance caused by semiconductor-metal transitions of ZnS (15 GPa) and GaAs (19 GPa).

It was necessary to confirm that the recovered sample did not contain other phases than garnet, particularly quench crystals of garnet from liquid, since the stability field of the (Mg,Fe)SiO_3 garnet phase is very narrow with respect to temperature at 20 GPa (*9*) and since there are some large temperature differences within the cylindrical heater. So, we made a thin section from a fragment

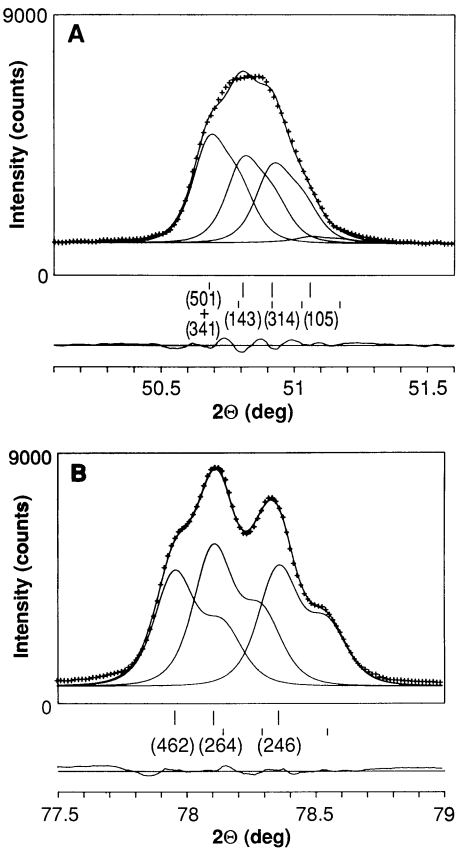

Fig. 1. Observed (plus signs) and calculated (solid line) x-ray powder diffraction profiles in the selected 2θ ranges for $MgSiO_3$ tetragonal garnet. The vertical bars underneath the pattern represent the positions of Bragg reflections (long bars: $K\alpha_1$, short bars: $K\alpha_2$), and the lower curve indicates differences between the observed and calculated intensities. (**A**) Portion of a quintuplet of diffractions from (501), (341), (143), (314), and (105). The diffraction from (501) and (341) are regarded as one peak because they have the same interplanar spacing. (**B**) Portion of a triplet of diffractions from (462), (264), and (246).

Table 2. Lattice parameters of (Mg,Fe)SiO_3 tetragonal garnets refined by the WPPD method. The values in parentheses are SDs in the least significant digit.

Material	*a* (Å)	*c* (Å)	*c/a*
$MgSiO_3$	11.5150(3)	11.4285(3)	0.9925
$(Mg_{0.90}Fe_{0.10})SiO_3$	11.5261(2)	11.4440(2)	0.9929
$(Mg_{0.81}Fe_{0.19})SiO_3$	11.5317(4)	11.4584(5)	0.9936

of the run product and examined it by optical microscopy and scanning electron microscopy before powdering the rest of the run product and examining it by x-ray diffraction. For the run products containing Fe, the low-temperature phase $(Mg,Fe)_2SiO_4$ (spinel) and SiO_2 (stishovite) were often found near both ends of the cylindrical sample in the coolest region during the run. In such cases, the garnet in the central, high-temperature region was carefully separated from the spinel and stishovite under the microscope. They can readily be distinguished from each other since the former is green whereas the latter has a rose color. Thin sections were also analyzed with an electron microprobe.

The x-ray intensity data of dust samples (1 to 3 mg) distributed on zero-background quartz plate sample holders were collected at room temperature on a powder diffractometer with an Fe rotating anode, with Mn-filtered Fe Kα ($K\alpha_1$: wavelength = 1.93597 Å, $K\alpha_2$: wavelength = 1.93990 Å), a divergence slit of 1°, and a receiving slit of 0.60 mm. The step-scan technique was used at a step interval of 1/72° over the 2θ range given in Table 1. The diffracted intensity was measured with a scintillation counter; NaCl powder was used as an internal standard. We corrected the peak shift caused by instrumental factors through WPPD refinement, using reflections from NaCl.

The diffraction pattern was indexed on the basis of a tetragonal unit cell and space group $I4_1/a$. Most diffraction peaks of the tetragonal garnet phase are heavily overlapping doublets, triplets, or combinations of them (Fig. 1). Figure 1A appears to be a single peak, but actually it is expected to be a quintuplet of the reflections from (501), (341), (143), (314), and (105). Such a complicated multiplet cannot successfully be decomposed into component Bragg reflections through individual profile fitting for a local powder pattern. In WPPD refinement, as shown in this figure, it was successfully decomposed. In the present study, the reflections that cannot be seen but might be underlying other reflections are included in analyses. As a result, the integrated intensity parameters of some peaks were determined to be zero (Table 1).

Lattice parameters and their least-squares

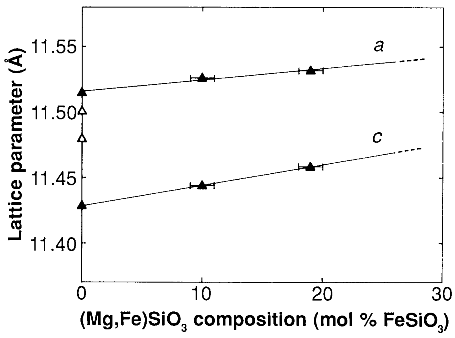

Fig. 2. Variation of lattice parameters *a* and *c* with composition in (Mg,Fe)SiO_3 garnets. Error bars represent SDs of the measurements of chemical composition. Open triangles indicate the results of the single-crystal analysis by Angel *et al.* (*5*).

SD values calculated by WPPD analyses are shown in Table 2. The powder patterns are well fitted, as shown by the low values of R_{wp} (weighted *R* factor), which is a conventional profile agreement index (Table 1). It is notable that the least-squares SD values are significantly smaller than the estimates of accuracy obtained from repetitions of the analysis; small changes in the starting parameters or process of the refinement, or both, would yield a variation in the refined lattice parameters greater than their SD values. The estimation of the true accuracy is very difficult, although the inferred error is several times as large as the SD. The end results given in Table 1 and 2 are the ones with the lowest values of R_{wp}.

The changes in lattice parameters with $FeSiO_3$ content are shown in Fig. 2. Both *a* and *c* increase linearly with Fe content. Angel *et al.* (*5*) synthesized a "single" crystal $MgSiO_3$ tetragonal garnet in which twins of micrometer scale were probably present and reported lattice parameters of *a* = 11.501(1) Å and *c* = 11.480(2) Å. Their measurements are not in agreement with our results; in particular, their value for the length of the *c* axis is about 0.05 Å larger than ours (Fig. 2). The reason for this discrepancy is not clear, although, as pointed out by them, it is possible that in the two samples the state of Si/Mg ordering in the octahedral sites may be different.

The powder pattern of $(Mg_{0.90}Fe_{0.10})SiO_3$ tetragonal garnet was very similar to that of $MgSiO_3$, and line splitting of overlapping reflections was very clear. For the powder pattern of $(Mg_{0.81}Fe_{0.19})SiO_3$ tetragonal garnet, on the other hand, line splitting was not clear except for the (400)-(004) doublet and the (240)-(402)-(204) triplet; other overlapping reflections were diffused and looked like one broad peak.

Under the optical microscope, sections of the tetragonal garnet phase exhibited low birefringence. In one of the runs on a starting material of $(Mg_{0.8}Fe_{0.2})SiO_3$ composition, an isotropic phase was optically detected; however, the x-ray diffraction pattern resembled that of tetragonal garnet that was synthesized from the same starting material, showing small splitting of some peaks. An electron microprobe analysis indicated that the chemical composition of this optically isotropic phase was also $x = 0.19(1)$ [where $x = Fe/(Fe + Mg)$], $Al_2O_3 \leq 0.1\%$ by weight, with no other contaminants present. The lattice parameters determined by the WPPD method are $a = 11.5323(3)$ Å and $c = 11.4541(4)$ Å, with $R_{wp} = 3.6\%$, which are essentially the values of isochemical tetragonal garnet. In conclusion, this "isotropic" phase is identified as tetragonal garnet. It may appear "isotropic" on account of the fineness of the crystal grain size. The microcrystallinity (<2 μm) is a remarkable microscopic feature of the tetragonal garnets synthesized in the present study.

Kato (*9*) reported in the conclusion of his experimental studies of the $MgSiO_3$-$FeSiO_3$ system that the cubic garnet phase with a normal garnet structure (majorite) is stable in the range of composition $0.2 < x < 0.4$ at 20 GPa and 2000°C, whereas the tetragonal garnet phase is stable for $x < 0.2$. We carried out a series of experiments with a starting composition of $x = 0.3$ as well but could not observe cubic garnet; we observed only a small amount of optically anisotropic tetragonal phase in insufficient proportions for x-ray diffraction analysis. The major proportion of the sample product was an assemblage of spinel and stishovite when experimental temperature was somewhat low and quench crystals from liquid when it was somewhat high. (The experiments were performed several times at temperatures around 2000°C.) Our present observations thus do not suggest the existence of the cubic garnet phase. It is possible that Kato (*9*) might have misidentified "isotropic" tetragonal garnet as "cubic" garnet.

REFERENCES AND NOTES

1. A. E. Ringwood and A. Major, *Earth Planet. Sci. Lett.* **12**, 411 (1971); M. Akaogi and S. Akimoto, *Phys. Earth Planet. Inter.* **15**, 90 (1977); L. Liu, *Earth Planet. Sci. Lett.* **36**, 237 (1977).
2. T. Kato and M. Kumazawa, *Nature* **316**, 803 (1985).
3. K. Fujino, H. Momoi, H. Sawamoto, M. Kumazawa, *Am. Mineral.* **71**, 781 (1986).
4. C. T. Prewitt and A. W. Sleight, *Science* **163**, 386 (1969).
5. R. J. Angel *et al.*, *Am. Mineral.* **74**, 509 (1989).
6. H. Toraya, *J. Appl. Crystallogr.* **19**, 440 (1986).
7. The WPPD method was referred to as whole-powder-pattern fitting without reference to a structural model (WPPF) when it was first presented by Toraya (*6*).
8. H. Sawamoto, *Phys. Chem. Minerals* **13**, 1 (1986).
9. T. Kato, *Earth Planet. Sci. Lett.* **77**, 399 (1986).

10. We are grateful to M. Kumazawa for continuous encouragement and helpful discussions. We also thank G. Fischer who reviewed the manuscript and S. Yogo for preparing thin sections of run products.

19 July 1989; accepted 17 November 1989

Effects on Carbon Storage of Conversion of Old-Growth Forests to Young Forests

MARK E. HARMON, WILLIAM K. FERRELL, JERRY F. FRANKLIN

Simulations of carbon storage suggest that conversion of old-growth forests to young fast-growing forests will not decrease atmospheric carbon dioxide (CO_2) in general, as has been suggested recently. During simulated timber harvest, on-site carbon storage is reduced considerably and does not approach old-growth storage capacity for at least 200 years. Even when sequestration of carbon in wooden buildings is included in the models, timber harvest results in a net flux of CO_2 to the atmosphere. To offset this effect, the production of lumber and other long-term wood products, as well as the life-span of buildings, would have to increase markedly. Mass balance calculations indicate that the conversion of 5×10^6 hectares of old-growth forests to younger plantations in western Oregon and Washington in the last 100 years has added 1.5×10^9 to 1.8×10^9 megagrams of carbon to the atmosphere.

DEFORESTATION HAS BEEN A source of increasing C in the atmosphere in the last century (*1–9*). However, it has recently been suggested that the CO_2 content of the atmosphere could be reduced if slowly growing, "decadent," old-growth forests were converted to faster growing, younger, intensively managed forests (*10*). Such suggestions may seem reasonable at first glance in that young forests have higher net primary productivity than old-growth forests (*11*). But such reasoning disregards the critical factor, which is the amount of C stored within a forest, not the annual rate of C uptake.

In this report, we explore the effects that conversion of old-growth to younger forests has on atmospheric CO_2 and terrestrial C budgets. We use three lines of evidence: the current disposition of C resulting from cutting old-growth timber, a model of C dynamics in old-growth and second-growth forests, and a comparison of C storage in an old-growth and a young forest by means of simulation.

Approximately 42% of the timber currently harvested in the Pacific Northwest enters long-term storage (products with a life-span of >5 years) in forms such as structural components of buildings (Fig. 1). This level is significantly higher than the historical level, which was as low as 20% in the 1950s (*12*). The long-term average is considerably lower than the current value because 75% of the timber harvested in the last 100 years in Oregon and Washington was cut before 1960 (*13*).

At least 15% of the wood fiber in a typical harvest is left behind as broken or defective (*14, 15*). Some of this material is used for fuel or paper production and is therefore quickly converted to atmospheric CO_2. Of the C removed from the site, 11% is in bark (*16*), which is either burned or composted to form mulch. Most of the tree volume removed from a stand is used in lumber production (*17*). When undecayed harvested wood is converted to boards or plywood, at least 35 to 45% is lost to sawdust or scrap during production (*15*). Some of this waste material is used in particle- and wafer-board production, but most is consumed as fuel or converted to paper. Production of paper, even with recycling, results in a loss of CO_2 to the atmosphere, in that only 46 to 58% of primary paper production is recovered as fiber (*15*) and the residue serves largely as fuel.

The result of all this activity is that, of the 325 Mg of C per hectare harvested from a typical old-growth forest, 187 Mg of C per hectare may be lost to the atmosphere from paper production, fuel consumption, or de-

M. E. Harmon and W. K. Ferrell, Department of Forest Science, College of Forestry, Oregon State University, Corvallis, OR 97331.
J. F. Franklin, U.S. Department of Agriculture Forest Service Pacific Northwest Forest and Range Experiment Station, Forestry Sciences Laboratory, Corvallis, OR 97331, and College of Forest Resources, University of Washington, Seattle, WA 98195.